

119516

20

*Library R.M.G.L.*

~~*C. F. J.*~~

TECHNICAL MEMORANDUMS  
NATIONAL ADVISORY COMMITTEE FOR AERONAUTICS

---

No. 486

---

✓ TANK TESTS OF TWIN SEAPLANE FLOATS

By H. Herrmann, G. Kempf, and H. Kloess

From Luftfahrtforschung, January 3, 1928

9.15  
9.2  
2.3  
2.5

---

Washington  
October, 1928



*Old copy*

NATIONAL ADVISORY COMMITTEE FOR AERONAUTICS.

TECHNICAL MEMORANDUM NO. 486.

TANK TESTS OF TWIN SEAPLANE FLOATS.\*

By H. Herrmann, G. Kempf, and H. Kloess.

The following report contains the most essential data for the hydrodynamic portion of the twin-float problem. Since no German data at all were available on this subject, we first investigated the means of adapting model-test results to full-sized floats. Accordingly, the following points were successively investigated:

1. Difference between stationary and nonstationary flow,
2. Effect of the shape of the step,
3. Effect of distance between the floats,
4. Effect of nose-heavy and tail-heavy moments,
5. Effect of the shape of the floats,
6. Maneuverability.

In order to keep in close connection with conditions in practice, the form of the Udet low-wing monoplane "U 10 a" was

\*"Schleppversuche an Zweischwimmerpaaren," from Luftfahrtforschung, January 3, 1928, pp. 18-30.- Joint report of the Deutsche Versuchsanstalt für Luftfahrt, Berlin-Adlershof (81st report) and of the Hamburgische Schiffbau-Versuchsanstalt, Hamburg 33 (46th report). This work, which reached the editor in December, 1926, is closely connected with the lecture on "Floats and Hulls," delivered by H. Herrmann (No. 14, of Zeitschrift für Flugtechnik und Motorluftschiffahrt, p. 126) and containing a systematic review of foreign publications with a partial use of the preliminary tests conducted at Hamburg (For translation, see N.A.C.A. Technical Memorandums Nos. 426 and 427.)

adopted for the flat-bottomed float. This float has a length of only 3.9 m (12.7 ft.) and consequently, the full-sized float can be towed in the water tank after being tested on the seaplane. The same lines were subsequently adopted for 7.2 m (23.6 ft.) floats. Owing to the fact that this seaplane was often flown by Herrmann, a close connection with conditions in practice has been maintained. We beg to express our thanks to the Udet Flugzeugbau (Udet Airplane Construction Company) which has supplied all the requisite models free.

The tests were carried out at the Hamburgische Schiffbau-Versuchsanstalt G.m.b.H. (Hamburg Shipbuilding Laboratory) where very high speeds can be reached owing to the great length of the water tank.

The Hamburg Shipbuilding Laboratory (H.S.V.A.)  
and the Installations for Making Float Tests

The H.S.V.A., built in 1913-15, was the result of the experience gained in Germany and abroad in the testing of ship models and exceeded in size all water tanks built up to that time. The length available for the tests extends over two tanks, respectively 8 m (26.25 ft.), and 16 m (52.5 ft.) wide, which merge into each other and have a total length of 350 m (1148 ft.). There are two electric carriages, of which the larger has a track gauge of 16.6 m (54.4 ft.), and can run the whole length of 350 m. It can reach a speed of 10 m/s (32 ft./sec.). However,

the speed in regular service should not exceed 8.5 m (27.8 ft.) per second, to avoid damaging the installation.

Among the devices installed on each carriage, those will only be considered which are used for resistance, immersion, and emersion measurements of ship or float models towed with corresponding speed. There are two methods of measuring the resistance in airplane-float tests. These methods are determined by the degree of accuracy of the measurements with float models on different scales.

1. The so-called resistance dynamometer, built for the usual ship-model tests, can measure resistances from 50 g to 12 kg (0.11-26.5 lb.). Owing to the fact that this testing installation is subject to a constant absolute error, the accuracy of the measurement is most satisfactory for large forces (8 to 12 kg), since the relative error then falls to 2%. With decreasing forces the relative error increases. The possibility of using the resistance dynamometer is strictly limited when floats of different size are tested. It was found that only resistances of float models of 1 to 1.5 m (3.2 to 4.9 ft.) in length could be measured with the above-mentioned satisfactory accuracy.

The test arrangement for the case considered is shown in Figure 1. The resistance dynamometer consists essentially of a lever oscillating freely on two knife-edges and having the shape of a balance beam W. On deflecting this beam, the force is tak-

en up by a tension spring or by the weight K. For accurate measurements the lever is inserted between two electric contacts e, which, as soon as they are alternately closed by the oscillating motion of the lever during the motion of the carriage, start a small electric motor which, according to its direction of rotation, tightens or loosens a spring especially designed for accurate measurement. This spring F carries a pen which plots its motions on a rotating drum covered with paper. In addition to this graphic representation of the resistance curve k during the motion of the floats, the time z and the path w are also electrically plotted on this drum. The time is measured by a stop watch and the distance by contacts distributed over the whole length of the tank at 2.5 m (8.2 ft.) intervals.

Two frames L are attached to the carriage and each frame can oscillate on two knife-edges. They are guided by two movable vertical rods S. The lower end of the measuring lever is connected to the model by a traction rod Z. It is attached to the front frame at the point where, in actual flight, the propeller thrust would take effect.

The twin floats and their supporting framework are attached at their front and rear ends to the two rods S and are thus free to immerse and emerge during the run. The degree of immersion and emersion is indicated by two pointers M, moving over a scale Sk secured to the carriage. The two rods are attached to two wires, each running over a pulley and supporting a weight

pan at its end. The twin floats are balanced by placing weights E on these pans sufficient to offset the lift of the wings, which increases as the square of the speed. The weight of the twin floats together with the supporting structure was counterbalanced by a weight G placed on a rod which passed through the center of gravity, so that, in spite of all the motions of the model during the run, the position of the center of gravity of the system was maintained.

2. It was found necessary to carry out tank tests with float models of different sizes and even with the full-sized float. As stated above, the resistance dynamometer has a limited capacity. Another method was developed for these tests, which likewise enabled the resistance to be directly weighed. (Fig. 2).

The twin floats are supported by two wires D running over two pulleys and placed at an arbitrary distance from each other. The other ends of these wires carry two weight pans on which the counterweights E are placed. In order to prevent lateral shifting, the floats are guided vertically by two rods S, the ends of which consist of two steel tubes R which are inserted into two sharp-edged slots N of the float support. The traction wire Z runs over two pulleys to a weight pan and is designed to offset the resistance. Moreover, a weak calibrated spring F is used for measuring smaller forces. The weight of the measuring pan is offset by a weight attached to the end of a

stretcher wire Sp running backward over two pulleys. The immersion and emersion is measured by the motion, over a fixed scale Sk, of pointers M attached to the stretcher wires.

Owing to the horizontal traction of the two wires, the traction wire Z on the one hand, and the stretcher wire on the other, the trimming of the model produces a nose-heavy moment. This moment naturally decreases with increasing distance between the model and the front and rear pulleys. In any case this moment can be compensated by a counter-moment as soon as the degrees of immersion and emersion are known.

This simple arrangement enables, according to its size, the measurement of forces from 0.01 to 200 kg (0.022-441 lb.). It is not subject to a constant absolute error, and the measurement, for four different sizes, is of an accuracy of 1 to 2%. The installation has given satisfactory results for floats 3.9 m (12.7 ft.), 1.95 m (6.4 ft.), and 0.4875 m (1.59 ft.) long.

The measurement during the test takes place in practically the same way with both arrangements. After completion of the model and the marking of the water line on the float, the model is weighed in the air. In order to reach the requisite displacement the model must be immersed to the water line by adding weights.

The test can be conducted in two different ways, either as an accelerated run with increasing speed, or at constant speed, which is surer for the taking of readings and for the evaluation

of the results. Both methods are described in the following paragraphs.

Scale Tests and Conversion from the  
Model to the Full-Sized Float

According to the actual propeller thrust developed during the take-off of a full-sized seaplane, the resistance of the floats is far from reaching the value which seems to result from model tests. This fact caused the large floats to be tested in the tank.

The value obtained by converting the resistance obtained in the first case with a 1/4-scale float model to the full-sized float was found to be actually 15% too high. (It is claimed abroad that 20 to 25% of the measured resistance is subtracted for the conversion of the model float tests to the full-sized float.) The experience gained from the model tests might have led to similar conclusions, since the values were converted to the full-sized float without subtracting the usual "Froude friction loss." But even in the case of the conversion with the subtraction of the friction, the figures could not be made to agree, since, according to Froude, this was only 50% of the measured resistance difference between the model and the actual float. This result led to the testing of different-scale models of the same float and the comparison of the results with the full-sized float and with one another. The logical result, according to



which the smallest float has the greatest resistance, is shown in Figure 3.

All four floats have lengthened steps, as shown in Figure 4. Besides, a progressive shifting of the resistance maxima is found to take place, so that the maximum value of the smallest model corresponds to the relatively highest Froude number. However, such a shifting of the critical Froude number can also be achieved by exerting a nose-heavy moment, as will be shown further on. Consequently, the model will be subjected during the run to a nose-heavy moment which must be a function of the resistance difference, i.e., of the relatively greater skin friction. Von Helmholtz, in the discussion of the writer's lecture delivered at the meeting of the W.G.L. in Düsseldorf in the summer of 1926, explained that this nose-heavy trim moment is due to "the increase in the model skin friction and to the increase in the thrust component acting high above the float and required to maintain the forces in equilibrium." The shifting of the critical Froude number causes a decrease in the angle of attack of the model and hence a difference in the relative flow, which disturbs the geometric and consequently also the dynamic similarity. Thus, although the reason for the resistance difference is to be attributed to the increased skin friction, it does not fully account for it and, as stated above, the usual friction corrections applied in model test practice are not sufficient to convert model test results to those for full-sized floats. In

addition to viscosity, capillary effects should also be taken into consideration.

The flow forces are influenced by gravity and viscosity and, according to the laws of the mechanics of similarity, it is quite impossible to obtain mechanical similarity of the model. When the Froude numbers agree, the Reynolds Numbers do not, and vice versa. Besides, it would be difficult to attain the speeds required by the Reynolds model law. It appears from the curves obtained by plotting the resistance coefficients against the Froude numbers, that the effect of gravity is preponderant before the float rises on the step, while the effect of viscosity preponderates afterwards during the planing period.

As a logical conclusion of the above explanation of the formation of the nose-heavy moment, which causes a shifting of the critical Froude numbers, one is led to attempt the estimation of the magnitude of the forces indicated above and of the possible capillary effects, by compensating the nose-heavy moment and, taking advantage of the resulting geometrical similarity of the model to the full-sized float, by suppressing the trimming effect of skin friction in the case of equal Froude numbers. Such tests are being carried out at the H.S.V.A. and reports on this subject will be published shortly.

## Stationary and Nonstationary State

The following method had been planned originally at Herrmann's suggestion. The model was to be towed with increasing speed, as is actually done for full-sized seaplanes. The wing lift was to be replaced by the lift of small airfoils in the water. In order to avoid errors due to inertia, the center of gravity had to be raised by adding weights, as is actually done with models. However, even without counterweights, a wooden model is so heavy that it has to be balanced. The whole mass and the part deducted for acceleration forces acting along the traction rod on the level of the propeller thrust were too large. The water resistance, instead of being derived directly, appeared as the difference of two rather large numbers. Difficulties were also encountered in plotting the tractive force, the velocity and the time curves. The driving gear of the carriage was designed for constant speed and not for uniform acceleration. Therefore, this idea had to be abandoned.

Its advantages are obvious. One single test run, carried out according to this method, would afford the same results as 8 to 20 tests by the usual method. Besides, a scale pan might be installed at the point of the model tail planes, and a chain, running over a recording wheel, might be dropped on it or removed its weight producing elevator deflections corresponding to the angle of attack of the floats. Finally, the dynamic process was

measured instead of a stationary one. As a matter of fact, stationary flow is of no interest in aircraft construction, but only a flow with steadily increasing velocity.

It was at least investigated as to how great the difference of the resistance was both with and without acceleration. The value lay at the limit of the measuring speed. This point can be actually disregarded in calculating the take-off time, which is the principal object of the tank test.

The flow lines in the water change but gradually with increasing speed. In the case of inherent acceleration, the floats always run with the flow lines of smaller speed. In case an unusually high acceleration should be produced by very strong engines, the water-resistance curve would be slightly shifted toward the left, i.e. the same resistances to small velocities. Of course this lagging behind can never lead to a practically manifest reduction of the take-off time.

#### Effect of the Shape of the Step

Experienced boat designers and other experts have often called our attention to the effect of the shape of the step. Figure 4 shows both the tested steps and the results obtained. As a matter of fact, the slight lengthening of the step toward the rear greatly affects the water resistance. It can be explained only by the better separation of the water at the step.

## Representation of Resistances

Owing to the peculiarity of Froude's law of similarity, it is very difficult to work out a general application of the result. All the measurements are converted to a displacement of 1000 kg (2204 lb.) at rest. Thus the resistance of different models can be easily compared. One should, however, always consider how heavily a float is loaded in proportion to its size. The angle of attack is always measured between the water line and the top of the float.

## Effect of Various Float Distances

In practice, the distance between the floats depends on the span, the height of the center of gravity and the distance of the lower wing above the water. Tests have been made in order to determine whether the water resistance is affected by a variation in the <sup>?</sup>latter distance. A distance of 1.8 m (5.9 ft.) for floats of 1 metric ton capacity each, corresponds to a wing span of approximately 9 m (29.5 ft.). In practice a corresponding, fully loaded seaplane usually has a span of from 10 to 11 m (32.8 to 36.0 ft.). With increasing size of the seaplane, the span and the distance between the floats increase as the square root of the weight when the wing loading remains unchanged, while the longitudinal dimensions of the float increase as the cube root, provided the load remains constant. Thus the dis-

tance between the floats increases as the square root, and their dimensions as the cube root of the total weight. This means that the floats, like the model, are separated further with increasing size.

According to Figures 5 and 6, a substantial effect can be traced on small models only. The result obtained with the 0.5 m (1.64 ft.) model shows that no tests should be made with such small models. The distance between floats does not affect the practical calculation of the take-off time, since the difference for the twin-float model was negligible.

#### Effect of Various Moments

The effect of various moments on the angle of attack and on the resistance is illustrated by Figure 7. It is seen that any displacement of the center of gravity, which may be considered as an interpretation of the moment, increases the resistance. Owing to the large nose-heavy moment, the float will be down by the head before reaching the critical speed. The measurements also afford a means for estimating the possible changes of trim produced by deflecting the elevator.

This circumstance likewise explains the difference between the result of the tank test and that of a full-sized float, since, owing to the high point of application of the thrust, the greater friction of the model can be considered as a nose-heavy moment. It changes the angle of attack and the resistance. As

soon as more data are available on this subject, we shall be able to decide on a change in the test arrangement, with a view to shifting the point of application of the thrust from the point where it acts on the model to the bottom of the float, the torque of the high-lying thrust being thereby replaced by a weight moment. No additional moment is then likely to arise and the conversion will be more accurate.

#### Effect of Various Float Shapes

The properties of various float shapes are illustrated by Figure 8. The lines of the three models are shown in Figures 9-11. All the measurements are given for a capacity of 1000 liters ( $1 \text{ m}^3$  or  $35.3 \text{ cu.ft.}$ ), regardless of the float type. This simplifies the calculations in designing. The sharp V-bottom float has been developed from <sup>the</sup> ordinary V-bottomed float by lengthening the bow to avoid the formation of spray. It is seen in Figure 19 that the water rises so high in front that it overlaps the propeller disk to a considerable extent. Figure 21 shows that this defect is eliminated by lengthening the bow. Besides, by causing strong impacts on rough water, the short V-bottom float is liable to compare unfavorably with the clean-cutting, sharp-nosed float. Therefore, the use of these lines is not recommended.

The flat-bottomed float is best suited for wood construction and the V-bottom keel types for metal construction. The bend in

the deck runs through to the last frame at the stern. In determining the weight, it should be taken into consideration that the V-bottom float may be less strongly built, since, on alighting, it is subjected to feebleness impacts. For equal strength the weight of the float may be considered proportional to its surface area. In this respect the float with the smallest water and air resistance is the most unfavorable, since it has the largest area. The advantage resulting from a reduced area of its frames, due to greater slenderness, is of little consequence.

TABLE I.

Comparative Figures for the Three Tested Models

All figures refer to a capacity of 1000 liters (35.3 cu.ft.).

Shape of Float Bottom		Flat	V-bottom	
			Ordinary	Pointed
Length	m	4.38	5.105	5.46
Distance of the c.g. above deck	m	1.28	1.36	1.33
" " " " forward of step	m	0.63	0.66	0.64
Elevation of thrust above step	m	1.75	1.84	1.84
Cross section of master frame	m <sup>2</sup>	0.348	0.282	0.266
Area of bottom from bow to step	m <sup>2</sup>	1.79	2.05	2.27
" " " " step to stern	m <sup>2</sup>	0.81	1.24	1.115
" " deck and sides	m <sup>2</sup>	4.66	5.11	5.20
Total area	m <sup>2</sup>	7.26	8.40	8.52



## Madelung's Representation

It is rather difficult to plot the characteristics of a pair of floats on a single diagram. According to Madelung, the result must be achieved by plotting the square of the speed. During the take-off, the weight of the floats is gradually assumed by the wings in proportion to the square of the speed. At the take-off speed the floats receive no support from the water. A straight line plotted in this diagram (Figs. 12-14) indicates for each speed, the weight supported by the water. Figures 12 to 14 are obtained by marking the points of equal resistance on a sufficient number of such lines and connecting them by curves. In order to facilitate comparison, the float resistance is expressed in fractions of the float capacity which is given a value of 1 metric ton for easier calculation of resistance and weight.

The diagram shows that, for an equal percental loading of the float, a definite resistance and angle of attack correspond to each load supported by the water at each speed. The water resistance is not affected by the manner in which this load is produced in each case by the difference between the displacement at rest and the wing lift. The value of the difference is determined in each case by the line.

A further step is taken in Figure 14 by plotting the angle of attack.

### Experimental Determination of Madelung's Diagram

The conditions chiefly considered of displacement at rest and take-off speed are tested first. The float is then balanced by weights according to the square of the velocity. If the result satisfies the requirements, the resistance and angle of attack are measured in terms of the speed for four constant loads. Thus four horizontal lines and one oblique line are determined in Madelung's diagram. These lines carry the points of equal resistance, which are then connected. At the same time the oblique line is a good check, since it cuts the horizontal lines. The resistance and the angle of attack must equal at the points of intersection, since the weight supported by the water and the speed are there equal.

### Differences of the Three Models

For various reasons the ratio of capacity to weight differed in all the tests. Consequently, additional diagrams must be plotted over Madelung's diagram (Fig. 8). This figure shows the considerable difference between flat and V-bottom floats. A slight suction effect is produced by the long gliding surface of the sharp-bottomed floats during the short period of constant speed required for the measurement, so that the usually sharp bend in the resistance curve is flattened out. In practice this defect is negligible, since, owing to the unstable flow

during the emersion, slight longitudinal vibrations are always produced, which let the water flow off smoothly. Herrmann, piloting a twin-float seaplane, has repeatedly maintained a constant critical speed by throttling the engine after emersion, but he was unable to avoid rather strong longitudinal vibrations by pulling and pushing the controls. The N.A.C.A. tests with a N-9 H seaplane were accompanied by similar phenomena.\* A good pilot can always be expected to keep the water-resistance curve below that of an ordinary V-bottomed float.

It must also be particularly emphasized that both the V-bottom floats were tested with the unfavorable step without the extended edge. This edge introduces a further improvement, which it is difficult to estimate until more accurate data are available.

Numerical Example of the Method of Calculating the  
Resistance and the Angle of Attack

Total weight of the seaplane  $G = 1700 \text{ kg}$

Take-off speed  $v = 25 \text{ m/s}$

Three float sizes are considered:

I. Capacity of each float  $J = 1500 \text{ kg}$

II. Capacity of each float  $J = 1700 \text{ kg}$

III. Capacity of each float  $J = 1900 \text{ kg}$

Adopted form: float with sharp keel.

---

\*Crowley and Ronan, "Characteristics of a Single-Float Seaplane during Take-Off." N.A.C.A. Technical Report No. 209. (1925)

The take-off speeds are first calculated according to the sixth root of the ratio of the float capacities. We are actually dealing with the capacities and not with the weights, since the capacity is the basis of the resistance in Madelung's diagram. These conditions are imperative on account of the Froude law.

$$v' = v \sqrt[6]{\frac{1.0}{J}}$$

$$\text{Float I} \quad v' = 25 \sqrt[6]{\frac{1.0}{1.5}} = 23.4 \text{ m/s}$$

$$\text{Float II} \quad v' = 25 \sqrt[6]{\frac{1.0}{1.7}} = 22.9 \text{ m/s}$$

$$\text{Float III} \quad v' = 25 \sqrt[6]{\frac{1.0}{1.9}} = 22.45 \text{ m/s}$$

We then determine the loading of the corresponding standard float of 1000 kg capacity

$$\text{Float I} \quad \frac{G}{J} 1000 = 1130$$

$$\text{Float II} \quad \frac{G}{J} 1000 = 1000$$

$$\text{Float III} \quad \frac{G}{J} 1000 = 895$$

We can now draw the three lines in Figure 14, from which the angle of attack and the resistance can be derived. The resistance is calculated by multiplying in each case the float capacity by the fractions given in the diagram. A reduction of 15% can be made owing to the fact that the model adopted has a length of 1.1 m. The result is shown in Figure 15. The differ-

ences are very small. The largest float has the smallest resistance. The take-off times can be calculated after determining the thrust available for acceleration.

### Flight Tests

Twin floats of a capacity of 2900 kg each were tested by Herrmann on the Starnberg lake. A metal propeller, producing a thrust of only 620 kg on the bench, was tested first. For an average loading, raising the total weight of the seaplane to approximately 2600 kg, the water resistance was about equal to the thrust. At first the seaplane was absolutely unable to take off without a strong head wind. The two floats were connected by two round tubes of 80 mm (3.15 in.) diameter. After carefully streamlining these tubes, the seaplane could take off without head wind in about 30 seconds with a full load of 2600 kg. After mounting a wooden propeller of 920 kg thrust, the take-off time, for the same load and a take-off speed of 80 km/h (50 mi./hr.), was reduced to 8-10 seconds. The take-off time for a total weight of 3000 kg was 22 seconds. The take-off time could be further reduced by substituting another propeller with greater thrust.

The seaplane had slotted wings and could take off and alight at two speeds. It could take off at 80 and 110, and alight at 70 and 100 km/h. With open slot and a low take-off speed the seaplane could take off with hardly any deflection of the ele-

vator, simply by adjusting the stabilizer correctly before starting and running the engine with wide-open throttle. The seaplane then began to climb smoothly. Unfortunately the result was quite different at 110 km/h. Little difference was noticed until the floats began to emerge, but the trouble began as soon as they rose on the steps. At 90 km/h the seaplane was so down by the head that the equilibrium could be maintained only by rapidly turning down the stabilizer. On pulling the control at 110 km/h the rear tip immersed, exerted a nose-heavy moment and caused the seaplane to tilt forward, calling for renewed pulling with subsequent immersion, tilting, etc., until a speed of 140 km/h was reached. When the seaplane was finally in the air, it shot up like a tail-heavy arrow. The take-off was usually completed at 120 km/h.

The pitching moment for the adopted position of the c.g., stagger, and decalage was extremely small. In order to achieve static stability, only very small horizontal tail planes were required. After completion, the c.g. was found to be 4-5 cm too far back. Consequently, there was static stability only when the propeller slip stream exerted a strong effect. Conditions were improved by considerably increasing the size of the elevator. The seaplane became statically stable under all conditions of flight. With closed slot the seaplane could now easily take off at 100 km/h. The acceleration after the take-off was also less pronounced. The change did not affect the take-off condi-

tions at low speed with open slot, since they had previously been quite satisfactory.

The changes, in comparison to the lines tested at the Hamburg tank were immaterial. The float designed for a capacity of 3200 kg was widened by cutting off a portion parallel to the deck. The resistance calculation had therefore to be based upon a capacity of 6400 kg for the two floats. This artifice was admissible, since the submerged part of the float remained unchanged. Furthermore, viewed from the side, the rear bottom was easily raised, so that a larger angle for pulling the control was available during the take-off than would have been the case if the lines had been strictly observed. In this connection the result was of all the more interest. For a take-off speed of 80 km/h, the angle of attack had to be from 18 to 20 degrees, and for 110 km/h, from 12 to 14 degrees only. It was easy to attain the larger angle at low speed, but difficult to attain the smaller angle at high speed. The seaplane was designed to take off at 80 km/h, while the speed of 110 km/h was to be developed only in case of emergency.

The high torque of the engine developing 620 HP. at 1500 R.P.M., depressed the left float and lightened the other, thereby considerably increasing the resistance of the left float. During the take-off without head wind, the seaplane tended to turn toward the left. For a 3000 kg loading of the 2900 kg floats, the seaplane could be taken off only with an initial

right-hand torque which, with a fully deflected rudder, gradually changed to the opposite direction. It was by increasing the size of the rudder. The torque was harmless when, the seaplane being flown empty, the float was not loaded above half its capacity.

### Maneuverability Tests

The maneuverability of the seaplane on the water proved to be very poor. It was slow to respond to the rudder. At the suggestion of the H.S.V.A., this property was tested on a model 1 m long. The test was based on the following consideration:

The turning capacity of the floats can be determined by exerting a constant moment and measuring the resulting deflection of the floats at various speeds. The arrangement of the test is shown in Figure 16.

The twin floats were suspended in the usual way on two wires carrying at their ends the scale pans with the corresponding counterweights E. The fulcrum point D was located in the immediate vicinity of the front point of suspension, while a scale G was installed at the rear point of suspension, where the deflection could be measured by means of a pointer Z secured to the carriage. A disk with a radius  $r$  was fastened to the front point of suspension. It was connected by two wires with two scale pans W located on the right and left sides of the twin floats. The float could be kept on the right course during the



run by compensating the drag. Lateral deflection was produced by placing a weight on one of the two scale pans. The tests were carried out twice at constant speeds until the beginning of the planing period, with a constant weight in each case.

As soon as the floats got off their course, the engendered moment of the value of the weight multiplied by the radius  $r$  of the disk was counterbalanced by a moment acting in the opposite direction and determined by the distance of the rear suspension wire from the fulcrum point  $D$  and by the counterweight. For the estimation of the test results this moment had to be deduced from the first moment. The moments, which were no longer constant on account of the different speeds, were plotted for each speed against the corresponding angle of deflection. Curves plotted in terms of the speed, transversely to this diagram, give a good idea of the maneuverability of the two models subjected to the comparative test (Fig. 17).

Everything is immediately explained by the result. Some pilots, when turning on the water, raced their engines, with the result that the increased speed prevented the completion of the turn. Other pilots turned with throttled engine at low speed. But even then the performances were not quite satisfactory and finally led to the Hamberg test. Figure 17 shows that, for a certain speed, which in practice is about the maximum admissible maneuvering speed, the turning capacity is considerably reduced, whereas the seaplane turns easier at low speed. A very strong

side wind requires a wide-open throttle in order to produce a sufficient moment of the vertical empennage, the speed on the water being thereby likewise increased. Then, of course, difficulties arise. The sharp, V-bottomed float, tested for comparison, presents no such unusual feature. These data afford means for calculating the turning capacity for side winds of different strength, when the requisite aerodynamical data are available.

#### Formation of Spray

The spray produced by a float increases with its resistance. In general, a float with low resistance produces little spray. The formation of spray decreases with decreasing load. The formation of spray is particularly characteristic of a float or hull with too short a bow. Conditions are improved by lengthening the bow. Figures 18-21 give a good idea of these conditions. The photographs were taken in such a manner that all three plates were exposed to the same flash of magnesium light. In the four exposures the three cameras occupied the same position. White painting of the floats is best suited for photographs. The moment when the photographs were taken is indicated in each of the three Madelung diagrams by a small circle.

Due to the propeller slip stream, the formation of spray of a full-sized seaplane differs from that of the model during the take-off. The spray is projected by the slip stream against the float struts and is again deflected by them. Moreover, the for-

mation of eddies and vortices contributes to atomize the rising water and to render its structure unrecognizable.

A good agreement with the model is often observed during alighting, although even then disturbances are frequently produced by the positive or negative thrust. Photographs like those of the model cannot be taken, since, in the water tank, the camera moves with the model, which enables a longer exposure. An exposure of  $1/200$  second produces quite a different picture from a time exposure or actual observation. It shows separate jets of water, as thick as a thumb, rising fountain-like, vertically in the air. The separate pictures of a motion-picture film which, in normal projection, produces the impression of a formation of spray similar to that of the model, likewise show the vertical projection of separate independent jets of water. As soon as these are mingled by the propeller slip stream, the similarity with the tank conditions is greatly reduced. However, the chief constructional data, such as the volume and height of the spray, can always be determined from the photographs, since the propeller slip stream and the float struts do not raise water from the sea but simply mix it up.

TABLE II.

Effect of Different Distances between Flat-Bottomed Floats  
Length of model 0.5 m (1.64 ft.)

Displacement at rest 1000 kg  
Total capacity of both floats 1900 "  
Capacity: weight  $2 \times 0.95$   
Angle at rest 3 degrees  
Lightening corresponding to a  
take-off speed of 87.8 km/h

Distance = 1.97 m			Distance = 2.56 m			Distance = 3.16 m		
v m/s	$\alpha$	W kg	v m/s	$\alpha$	W kg	v m/s	$\alpha$	W kg
4.55	4.1	166	4.43	4.2	166	4.49	3.8	159
5.80	4.5	192	5.10	4.2	180	5.11	4.2	182
5.84	4.7	217	5.69	4.5	210	5.75	4.3	213
6.35	4.2	236	6.32	4.7	231	6.37	4.7	239
6.70	4.2	254	6.71	4.7	255	6.70	5.2	262
7.06	4.5	282	7.03	4.8	282	6.96	5.2	282
7.35	5.2	300	7.22	5.5	311	7.29	5.0	306
7.64	5.0	334	7.71	6.0	357	7.60	5.7	353
7.88	6.5	358	8.00	7.3	385	7.88	5.5	392
9.04	7.3	330	8.32	7.3	348	8.23	7.5	361
9.47	7.3	305	8.61	7.7	348	8.57	8.0	357
10.03	7.3	285	9.62	7.3	313	9.25	8.0	327
10.06	6.7	278	10.06	7.3	292	10.15	8.0	306
10.54	6.3	269	10.45	7.3	275	10.45	7.3	296
11.46	6.3	251	11.12	6.2	257	11.07	6.7	269
12.25	6.2	233	11.69	6.2	250	11.62	6.0	260
12.91	6.2	220	12.34	6.2	257	12.20	6.3	251
13.45	4.8	215	12.99	6.5	250	13.70	4.8	224
14.75	4.2	206	13.63	5.5	249	14.90	4.8	207
15.36	3.8	179	14.71	4.2	215	15.75	4.2	219
16.20	3.7	179	15.45	4.2	206	17.33	3.2	251
18.40	3.2	179	17.21	4.2	170	18.50	3.0	206
8.48	5.0	353	19.88	4.2	134	4.08	7.3	297
17.13	3.2	171	13.19	5.5	233	18.6	3.7	233
19.4	-	153				18.9	3.7	203
7.96	7.2	359				20.7	3.2	125
						18.4	4.0	211

TABLE III.

Effect of Different Distances between Flat-Bottomed Floats  
Length of model 2.0 m (6.56 ft.)

Displacement at rest 1000 kg  
Total capacity of both floats 1900 "  
Capacity: weight  $2 \times 0.95$   
Lightening corresponding to a  
take-off speed of 87.8 km/h

Distance = 1.97 m			Distance = 2.56 m		
v m/s	$\alpha$	W kg	v m/s	$\alpha$	W kg
5.23	3.3	177	5.39	3.5	189
5.62	3.5	194	5.85	3.7	210
5.93	3.5	205	6.23	3.7	227
6.28	3.7	219	6.60	4.0	265
6.44	4.0	238	6.90	4.2	266
7.46	4.3	295	7.36	4.3	294
7.86	4.5	294	7.44	4.3	300
7.66	4.3	305	8.10	4.3	284
8.28	4.5	280	8.41	4.2	272
8.57	4.3	269	9.20	4.2	238
9.19	4.2	238	9.81	4.2	219
10.34	4.2	210	7.17	4.2	273
11.05	3.8	182			
7.29	4.3	301			
7.17	4.2	301			
6.86	4.0	252			
6.64	4.0	252			
7.44	4.3	301			
7.66	4.3	297			

TABLE IV.

## Flat-Bottomed Float Resistance with Constant Lightening

Displacement at rest 1000 kg

Capacity of both floats 1900 "

Capacity: weight 2 x 0.95

Distance 1.97 m

Lightening = 0 kg		Lightening = 224 kg		Lightening = 448 kg		Lightening = 672 kg	
v m/s	W kg	v m/s	W kg	v m/s	W kg	v m/s	W kg
4.81	186	4.75	139	4.85	198	4.58	98.5
6.34	254	6.20	180	6.32	167	6.17	131.5
7.76	420	7.87	322	7.82	236	7.66	168
9.74	257	9.69	294	9.74	206	9.48	150
11.11	290	11.06	250	11.22	205	11.00	152
12.35	268	12.33	233	12.49	213	12.22	161
14.05	273	13.78	236	13.79	224	13.39	139
17.14	259	15.48	233	17.05	187	15.40	149
6.66	268	6.67	227	14.41	187	17.07	143
7.21	315	7.27	277	13.89	187	18.10	154
8.16	411	8.19	325	15.52	179	6.72	161
8.92	395	9.01	299	18.49	175	7.30	164
				6.67	194	8.23	187
				7.30	219	9.09	172
				8.20	250		
				9.00	228		

Effect of Longitudinal Moments on the Resistance and  
Angle of Attack of a Flat-Bottomed Float.  
Length of model 0.5 m (1.64 ft.)

Distance between floats 1.97 m

Tail-heavy moment of 334 mkg Angle at rest 6.15 deg.			Nose-heavy moment of 334 mkg Angle at rest 0 deg.			Tail-heavy moment of 166 mkg Angle at rest 4.75 deg.			Nose-heavy moment of 166 mkg Angle at rest 1.25 deg.		
v m/s	$\alpha$	W kg	v m/s	$\alpha$	W kg	v m/s	$\alpha$	W kg	v m/s	$\alpha$	W kg
6.48	9.7	282	6.55	1.5	278	5.81	7.6	224	5.81	3.7	224
7.26	12.7	362	10.10	2.5	367	6.92	8.75	280	6.93	4.0	278
7.58	12.7	367	10.97	2.5	331	7.60	9.75	385	7.67	3.7	323
7.88	13.3	367	11.53	1.8	318	8.37	10.25	385	8.46	4.7	421
8.65	12.7	331	12.30	1.0	296	9.15	10.25	342	9.15	4.7	399
9.44	12.7	302				9.80	10.25	313	9.80	4.7	376
10.10	12.4	288				10.67	9.75	291	10.67	4.7	349
10.97	12.0	268				11.40	8.25	255	11.40	4.0	313
11.53	12.0	241				12.13	9.75	233	12.13	4.0	277
12.30	10.8	224				8.14	7.25	367	7.84	1.5	340
6.55	10.2	287				7.88	5.75	402			
7.07	10.2	313									

TABLE VI.

## Flat-Bottomed Float Resistance with Constant Lightening

Displacement at rest                      1000 kg  
 Capacity of both floats                    1900 "  
 Capacity: weight                            2 x 0.95  
 Distance                                      1.97 m

Lightening 0 kg		Lightening = 224 kg		Lightening = 448 kg	
v m/s	W kg	v m/s	W kg	v m/s	W kg
5.65	207	5.86	174	5.30	128
6.39	248	5.57	174	6.17	145
7.40	336	6.41	201	7.05	171
8.25	329	7.24	244	7.90	155
9.18	294	8.04	247	8.75	144
9.96	266	8.93	219	9.35	133
		9.65	199	10.17	126
		10.80	189	10.95	123
				12.15	119



TABLE VII.

Flat-Bottomed Float Resistance with Variable  
and Constant Lightening  
Length of model 1.0 m (3.28 ft.)

Displacement at rest                      1000 kg  
Capacity of both floats                    1900 "  
Capacity: weight                            2 x 0.95  
Distance                                      1.97 m

Lightening corresponding to a take-off speed of 87.8 km/h			Lightening constant = 0 kg		Lightening constant = 224 kg		Lightening constant = 448 kg	
v m/s	$\alpha$	W kg	v m/s	W kg	v m/s	W kg	v m/s	W kg
6.01	4.0	134	4.37	185	4.39	151	4.08	90
6.45	4.2	276	5.36	219	5.40	180	5.64	122
7.41	5.5	329	6.39	275	6.39	219	6.47	159
8.05	5.3	310	7.79	341	7.50	247	7.66	147
8.54	5.7	296	9.49	341	8.52	229	8.97	124
9.26	5.3	253	9.40	291	9.48	196	10.07	124
9.81	5.0	245	10.42	257	10.60	179	11.24	123
10.64	4.8	217			11.50	185	12.24	118
11.22	4.5	210			14.25	163	13.39	112
4.11	4.0	162					15.58	106
4.89	3.7	173						
5.40	3.7	189						
6.08	4.0	252						
6.65	4.5	258						
7.29	5.3	308						
7.76	4.5	303						
6.67	3.5	280						
7.52		317						
8.75		272						

TABLE VIII.

Resistances of the Obtuse or Ordinary V-Bottom Float  
with Variable and Constant Lightening  
Length of model 1 m

Displacement at rest 1000 kg  
Capacity of both floats 1680 "  
Capacity: weight  $2 \times 0.84$   
Angle at rest 3 degrees  
Distance between floats 1.97 m

Lightening corresponding to a take-off speed of 87.8 km/h			Lightening constant = 0 kg		Lightening constant = 224 kg		Lightening constant = 448 kg	
v m/s	$\alpha$	W kg	v m/w	W kg	v m/s	W kg	v m/s	W kg
3.99	4.2	112	4.54	129	3.96	79	3.96	56
4.53	4.1	124	5.04	146	5.04	137	5.09	79
5.06	3.8	140	6.31	186	6.25	146	6.25	90
5.75	3.8	152	7.45	225	7.45	174	7.45	107
6.31	3.5	180	8.45	214	8.45	152	8.45	101
6.90	4.2	202			9.75	146	9.75	95
7.48	4.5	191			10.93	135	10.93	90
8.08	5.3	180						
8.69	6.2	162						
9.31	6.8	163						
8.89	7.2	157						
11.03	7.3	146						
12.12	7.3	124						
5.73	3.8	163						

TABLE IX.

Resistances of the Sharp-Bottomed Float for  
Variable and Constant Lightning  
Length of model 1.1 m (3.6 ft.)

Displacement at rest	1000 kg
Total capacity of both floats	1830 "
Capacity: weight	$2 \times 0.915$
Angle at rest	3 deg.
Distance between floats	1.97 m

Lightening correspond- ing to a take-off speed of 87.8 km/h			Lightening constant = 0 kg			Lightening constant = 224 kg			Lightening constant = 448 kg		
v m/s	$\alpha$	W kg	v m/s	$\alpha$	W kg	v m/s	$\alpha$	W kg	v m/s	$\alpha$	W kg
4.30	4.1	107	4.27	5.0	110	4.30	3.2	92	4.19	4.3	61
4.75	4.5	118	5.38	4.8	142	5.40	4.1	112	6.45	4.0	96
5.38	4.2	129	6.39	5.2	178	6.50	4.0	135	8.90	7.3	118
5.93	4.0	146	7.60	7.7	214	7.65	5.2	152	11.25	7.3	124
6.52	3.3	169	8.73	10.0	217	9.00	8.4	169	11.95	7.3	110
7.09	4.2	186	9.97	10.3	214	10.00	9.5	169	16.10	4.5	107
7.58	5.3	191	12.12	10.0	207	11.28	10.0	155			
8.25	6.5	197	13.50	9.2	191						
8.90	7.3	191									
9.45	7.8	191									
10.10	7.7	180									
11.18	7.3	163									
12.37	6.8	146									
13.56	6.2	135									
7.69	5.3	202									

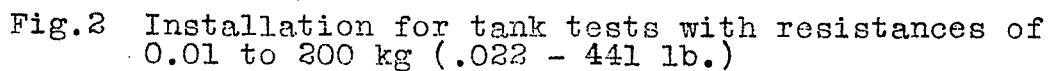
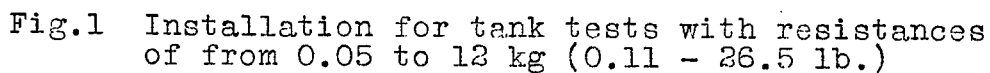
TABLE X.

## Maneuverability Tests

Float bottom	Flat	Sharp, V-bottom
Displacement at rest	1000 kg	1000 kg
Total capacity of both floats	1900 kg	1830 kg
Capacity, weight	2 x 0.95	2 x 0.915
Lightening corresponding to a take-off speed	87.8 km/h	87.8 km/h
Distance between floats	1.97 m	1.97 m
Length of model	1.0 m	1.1 m

Flat-Bottomed Float			Sharp, V-Bottomed Float		
Velocity m/s	Torque m/kg	Angle deg.	Velocity m/s	Torque m/kg	Angle deg.
4.35	27.4	2.0	4.35	22.8	4.0
5.41	30.5	1.5	5.44	28.8	2.8
6.60	36.8	0.75	6.56	34.9	1.5
7.74	28.4	1.75	7.65	36.6	1.3
8.90	25.8	2.0	8.86	37.6	1.0
4.41	59.3	3.0	4.38	54.0	6.0
5.50	68.3	2.0	5.46	66.7	3.8
6.71	75.6	1.0	6.62	74.0	2.3
7.74	56.3	3.5	7.65	76.9	1.8
8.94	52.6	3.5	8.86	77.1	1.5

Translation by W. L. Koporinde, Paris Office,  
National Advisory Committee for Aeronautics.



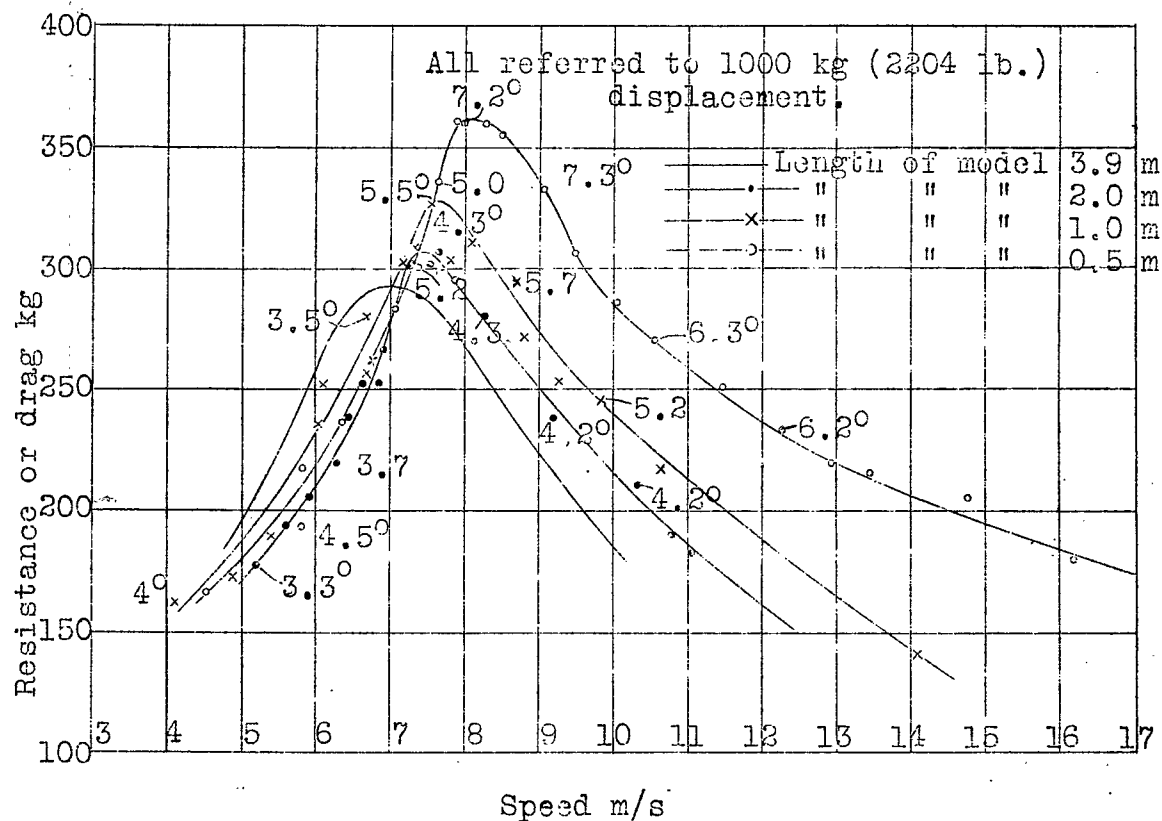


Fig. 3 Comparison of resistances measured on geometrically similar models 0.5, 1.0, 2.0, and 3.9 m (1.64, 3.28, 6.56, 12.8 ft.) long. Take off speed 87.7 km/h (54.5 mi/hr.).

- A, Load-reduction constant = 0    Difference = 12% +  
 B, Load-reduction constant = 224 kg    Difference = 22% +  
 C, Load-reduction constant = 448 kg    Difference = 32% +  
 D, Variable load reduction corresponding to take-off  
 speed 87.8 km/h. Difference = 11% +

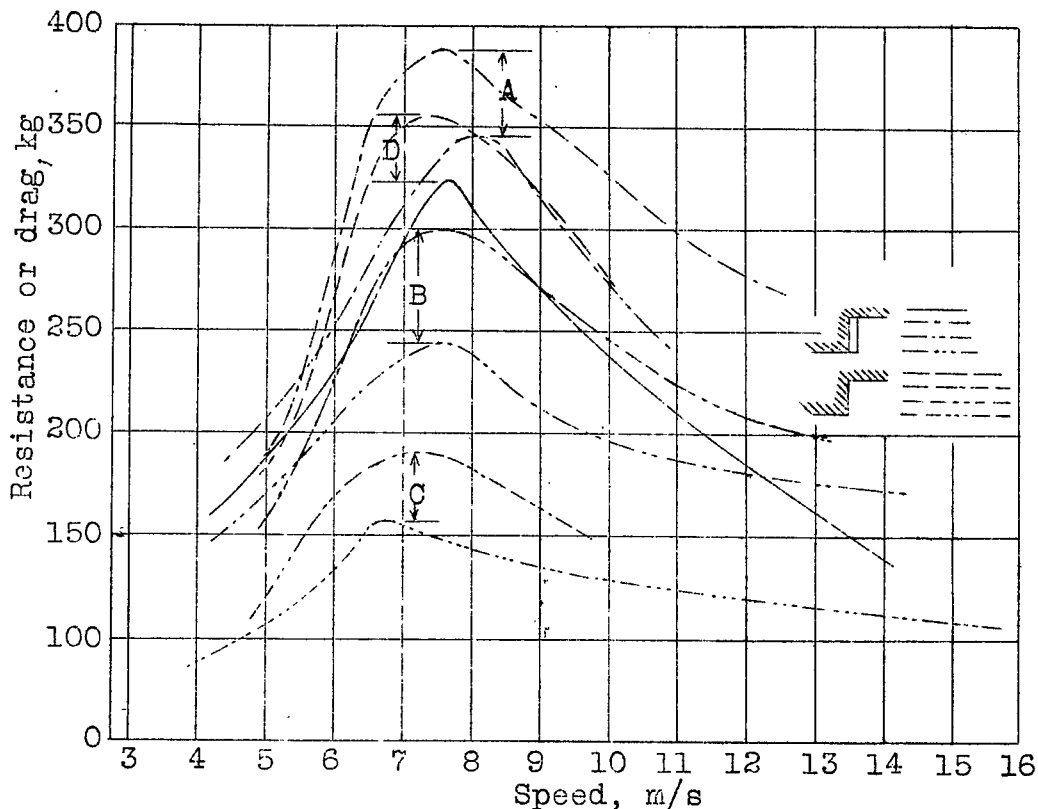


Fig.4 Effect on the water resistance of the shape of the step of a flat-bottomed float.

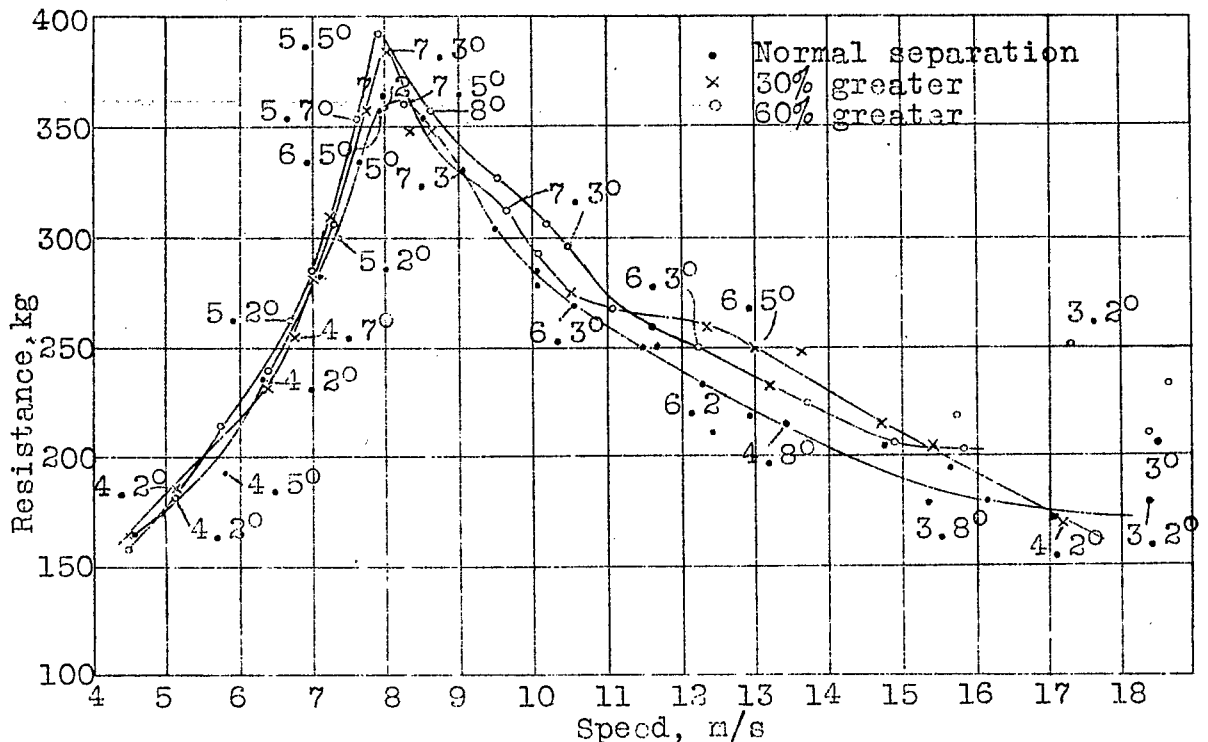


Fig. 5 Influence on the water resistance of the distance between flat-bottomed floats. Model 0.5 m (1.64 ft.) long.

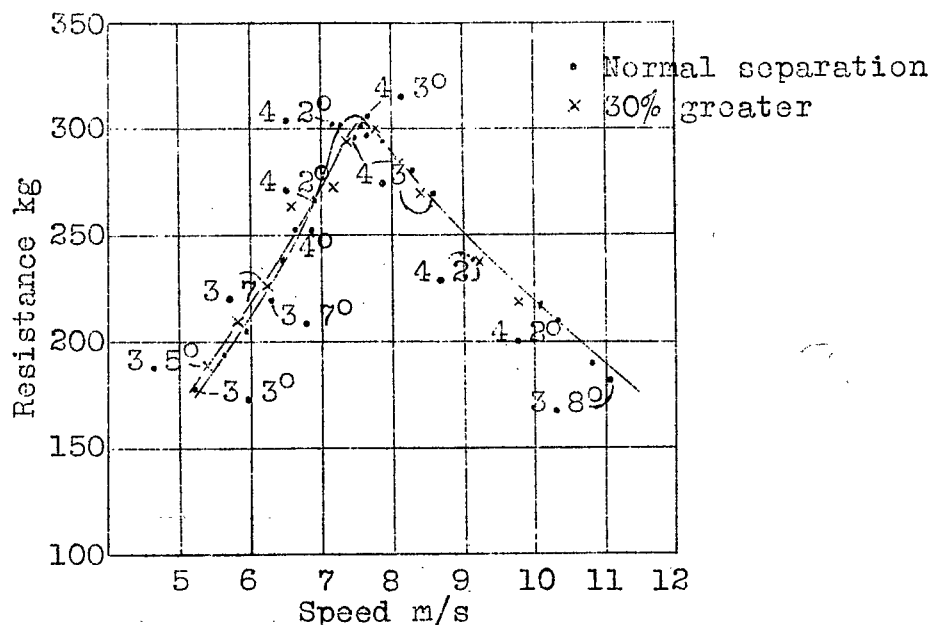


Fig. 6 Influence on the water resistance of the distance between flat-bottomed floats. Model 2.0 m (6.56 ft.) long.



- Exp. 1479 No moment                      + Exp. 1493 Nose-heavy mom.  
 × " 1492 Tail-heavy moment              ○ " 1489 Tail " moment  
 ○ Exp. 1491 Nose-heavy moment

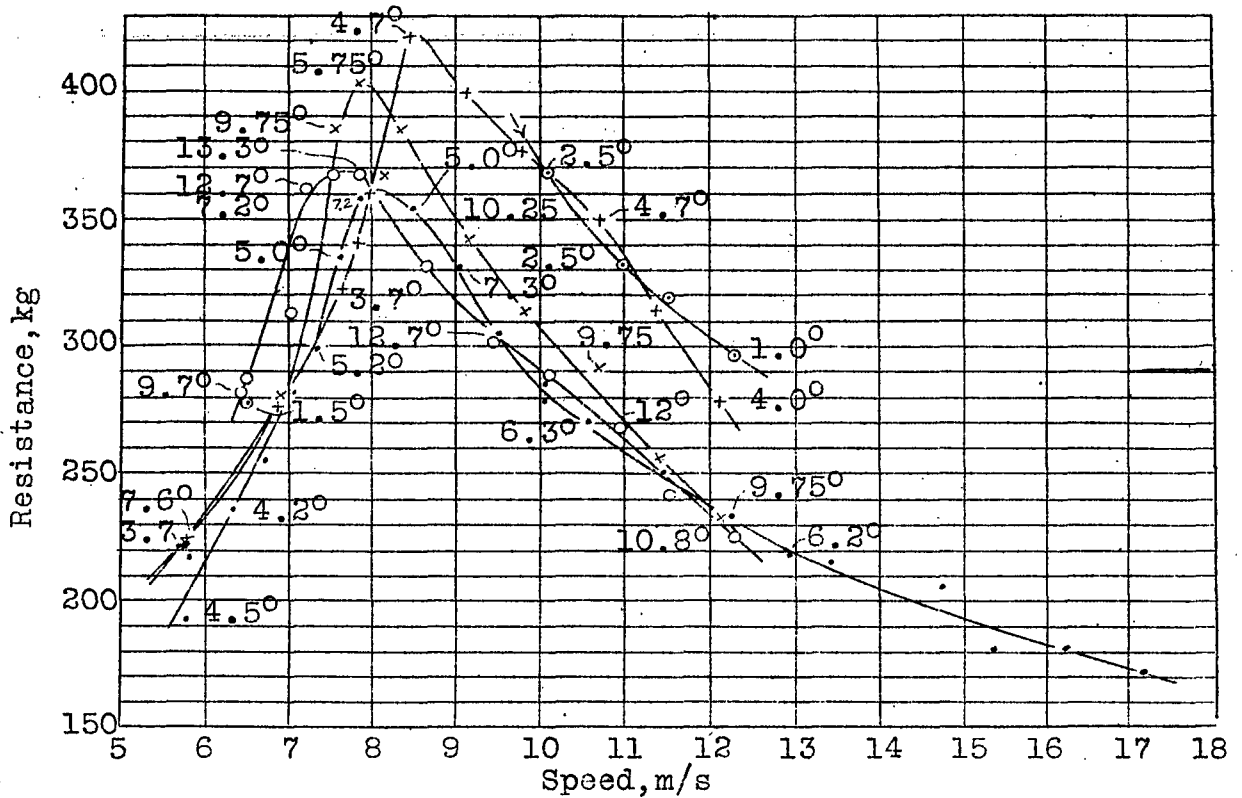


Fig.7 Effect of the longitudinal moment on the resistance and angle of attack of a 0.5 m flat-bottomed float model. Exp.,1479

no moment. Exp.,1492  
 Tail-heavy moment  
 166 mkg. Exp.,  
 1493 Nose-heavy  
 moment 166 mkg.  
 Exp., 1489  
 Tail-heavy  
 moment 334 mkg.  
 Exp., 1491  
 Nose-heavy  
 moment 334 mkg

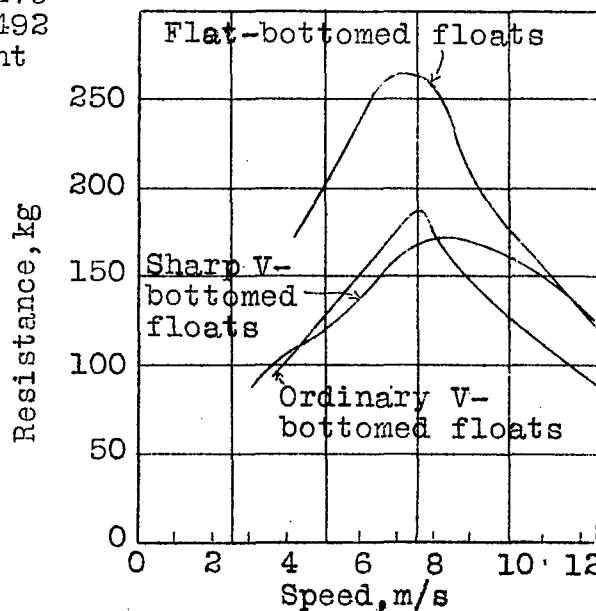


Fig.8 Resistance of the 3 tested floats for a seaplane of 1.0 ton total weight, 2.2 tons capacity of the two floats and 80 km/h take-off speed.

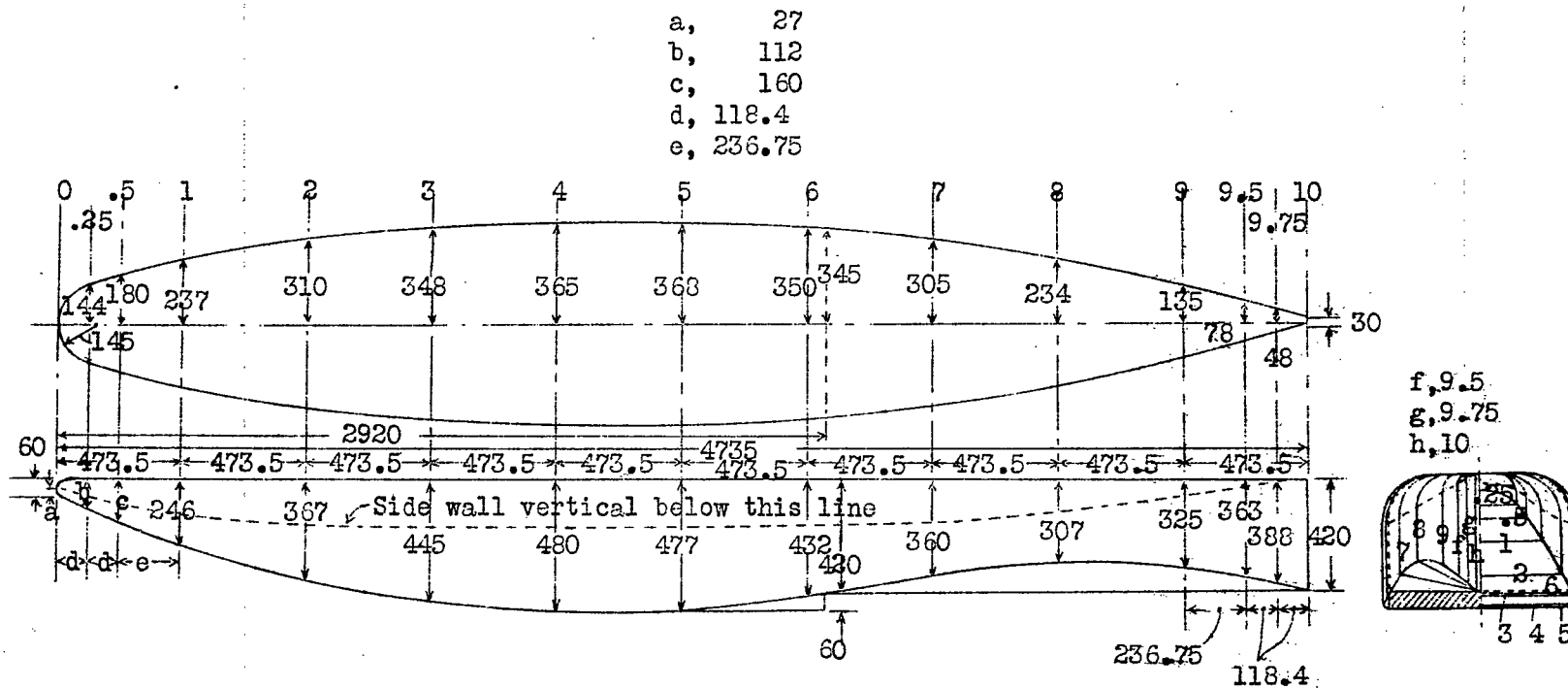
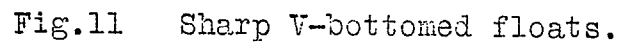


Fig.9 Flat-bottomed floats.

- [illegible]

Fig.10 Ordinary V-bottomed floats.



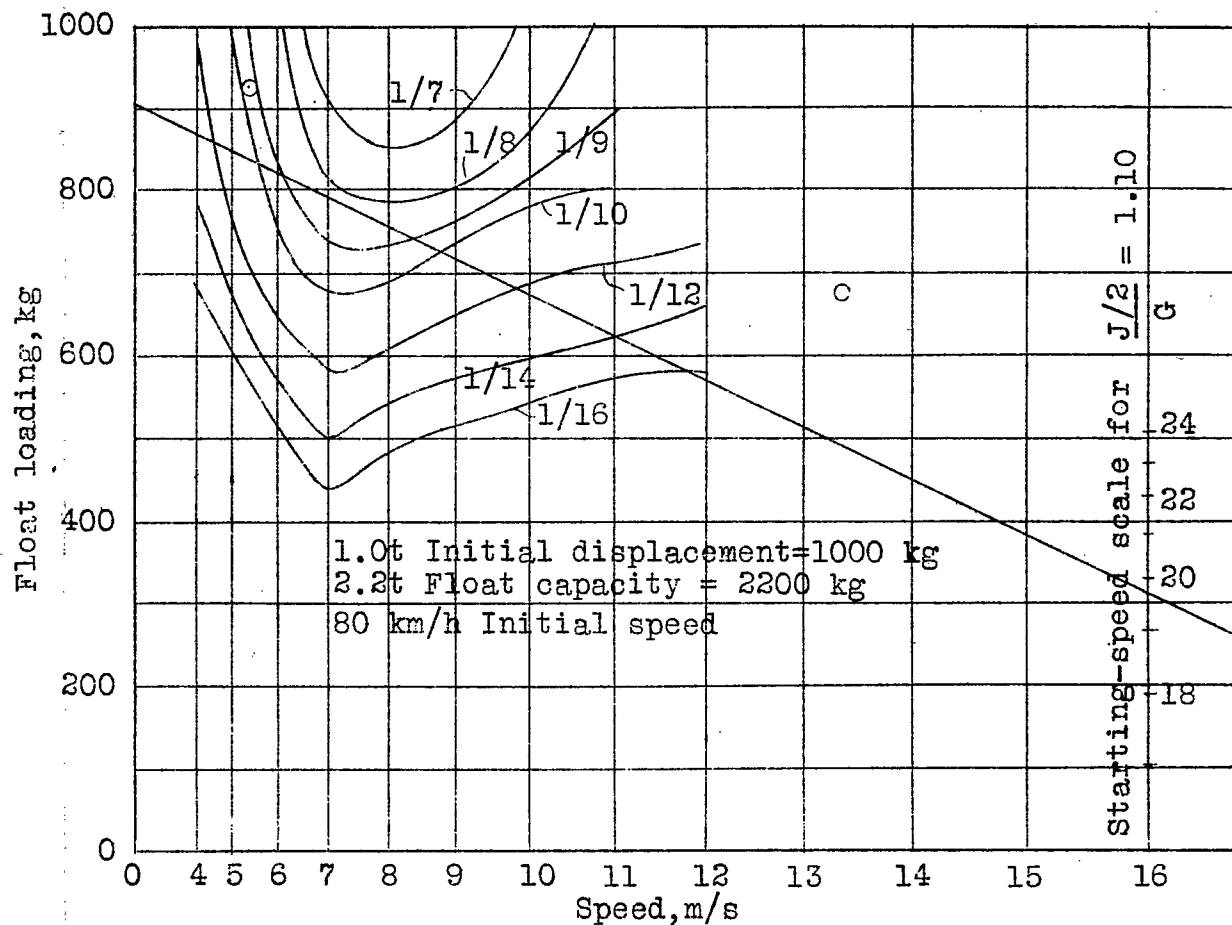


Fig.12 Madelung's resistance diagram of a flat-bottomed float, measured on a model 1.0 m long. The two circles correspond to the moment when Figs.19 and 21 were photographed. Flat-bottomed float, 2000 liters capacity of pair of floats. (2000 liters =  $2 \text{ m}^3 = 70.63 \text{ cu.ft.}$ )

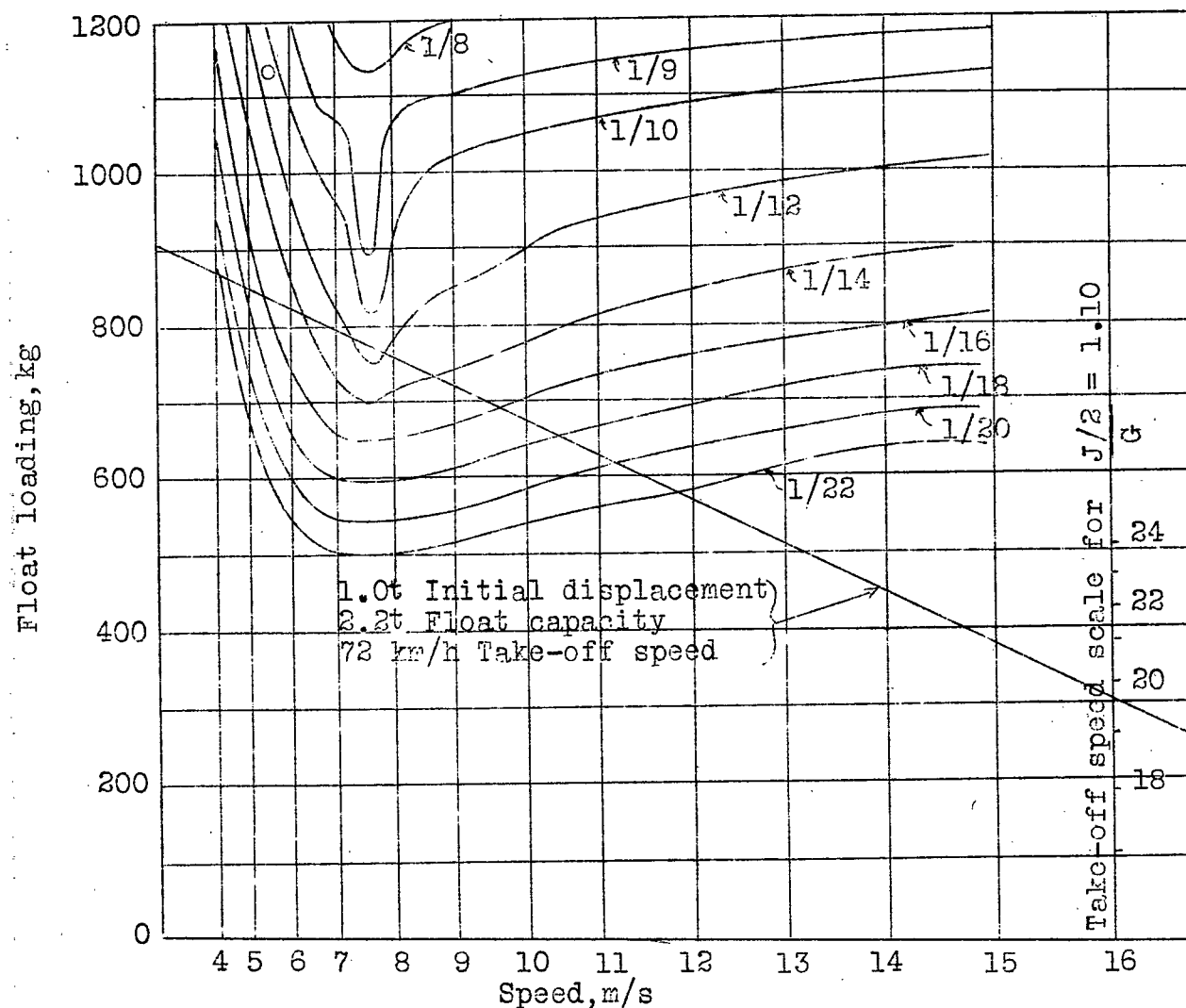


Fig.13 Madelung's representation of the resistance of an ordinary V-bottomed float, measured on a model 1.0 m long. The circle corresponds to the time of Fig.18. Ordinary V-bottomed float, 2000 liters capacity of pair of floats. (2000 liters =  $2 \text{ m}^3 = 70.63 \text{ cu.ft.}$ )

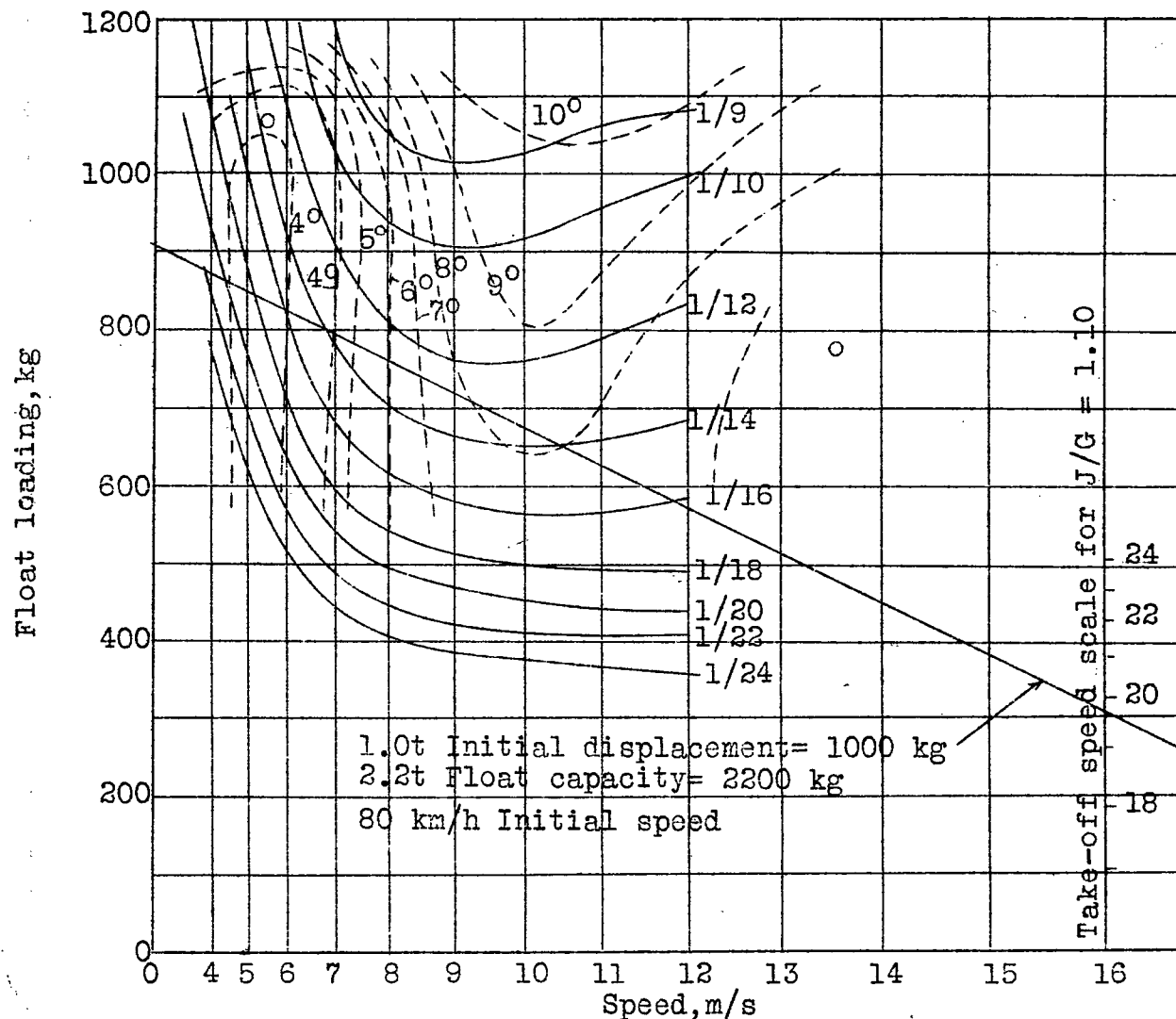


Fig.14 Madelung's resistance and angle of attack diagrams for the sharp V-bottomed float. Measured on a 1.1 m model. The two circles correspond to the time of Figs.20 and 22. Sharp V-bottomed float. 2000 liters capacity of pair of floats. (2000 liters =  $2 \text{ m}^3 = 70.63 \text{ cu.ft.}$ )

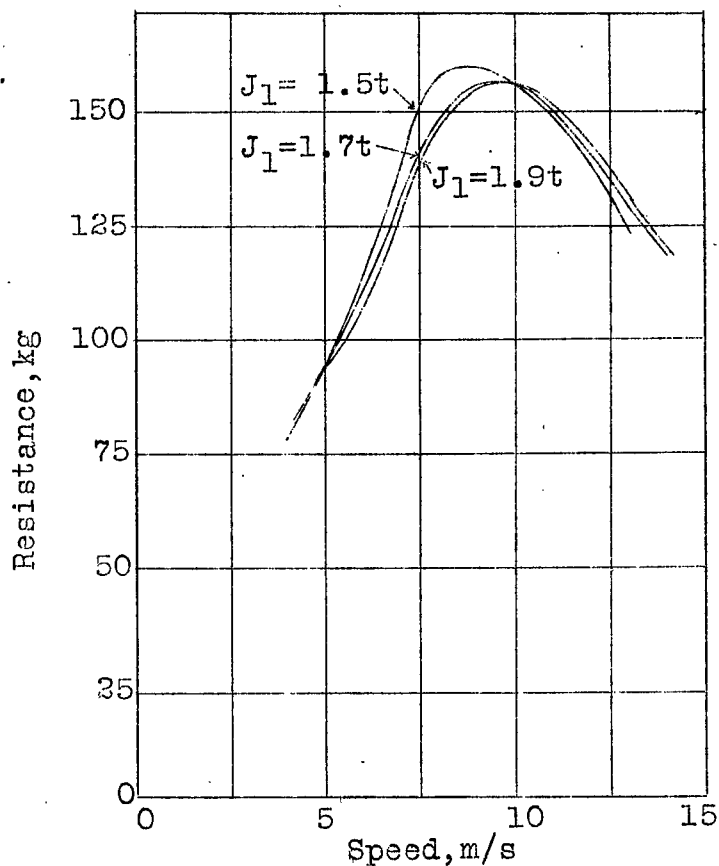


Fig.15 Resistance of the sharp V-bottomed float, for 3 float sizes and the same weight of the seaplane. 15% can be deducted from the resistance for conversion from the model to the full-sized float.



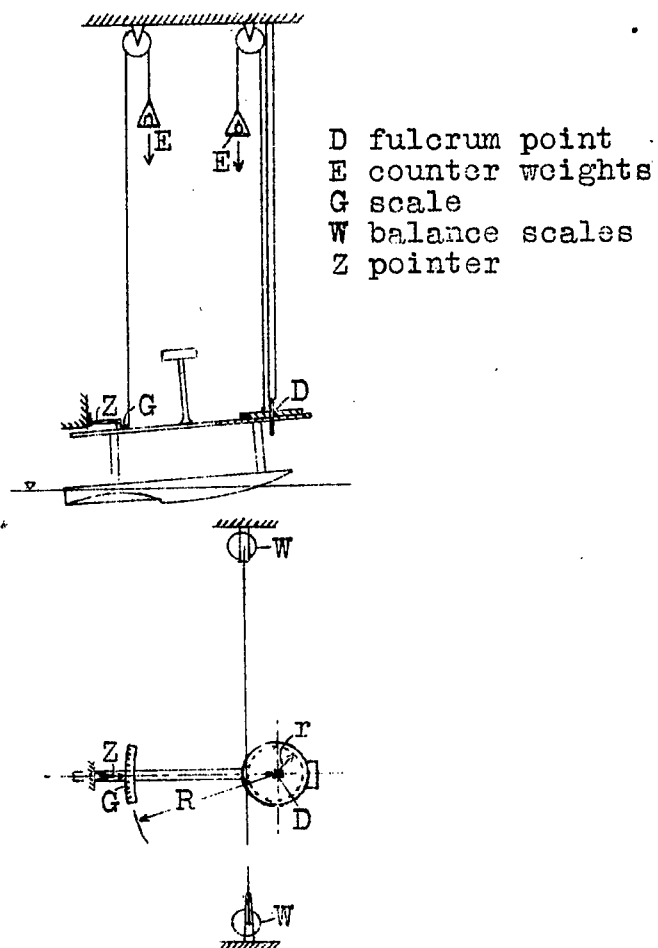
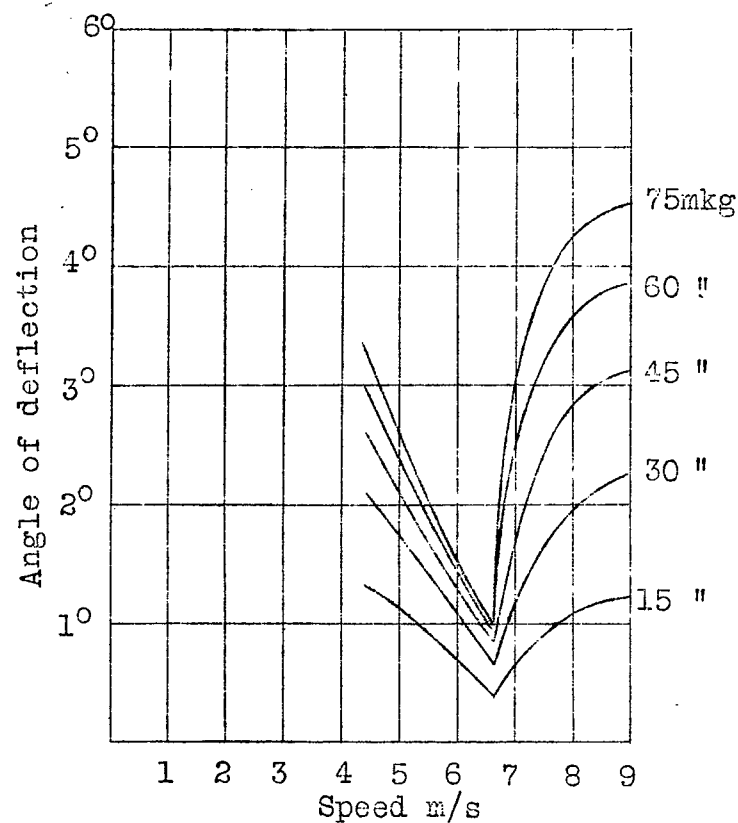


Fig.16 Installation for maneuverability tests.

Flat-bottomed float model. Length = 1 m



Sharp V-bottomed float model  
Length 1.1 m

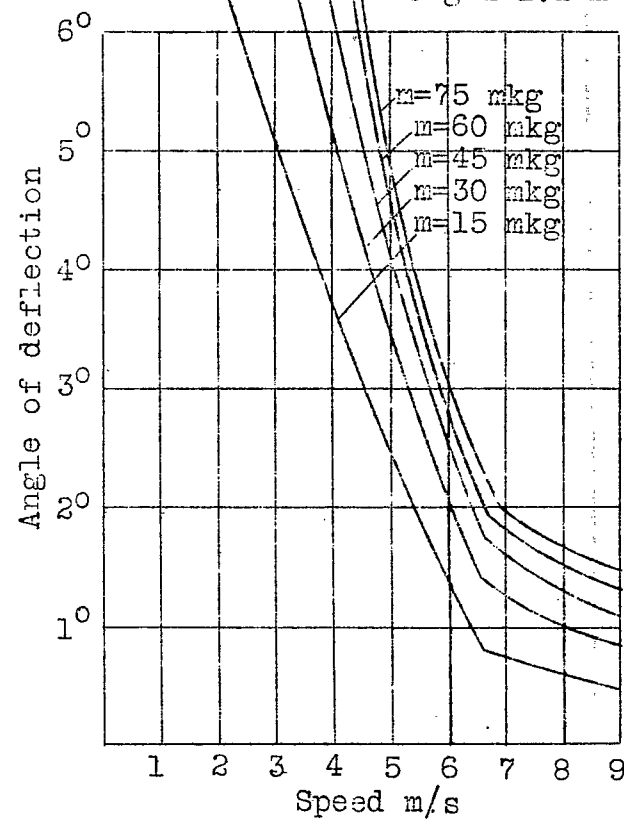


Fig.17 Maneuverability test result referred to a displacement of 1000 kg.

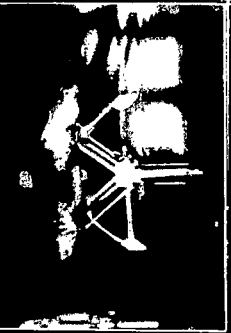
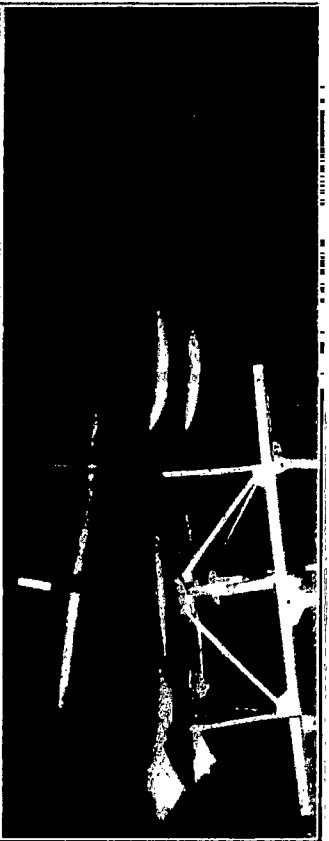


Fig. 18 Formation of waves about flat float at low speed. Length of model 1 m, velocity 2.44 m/s

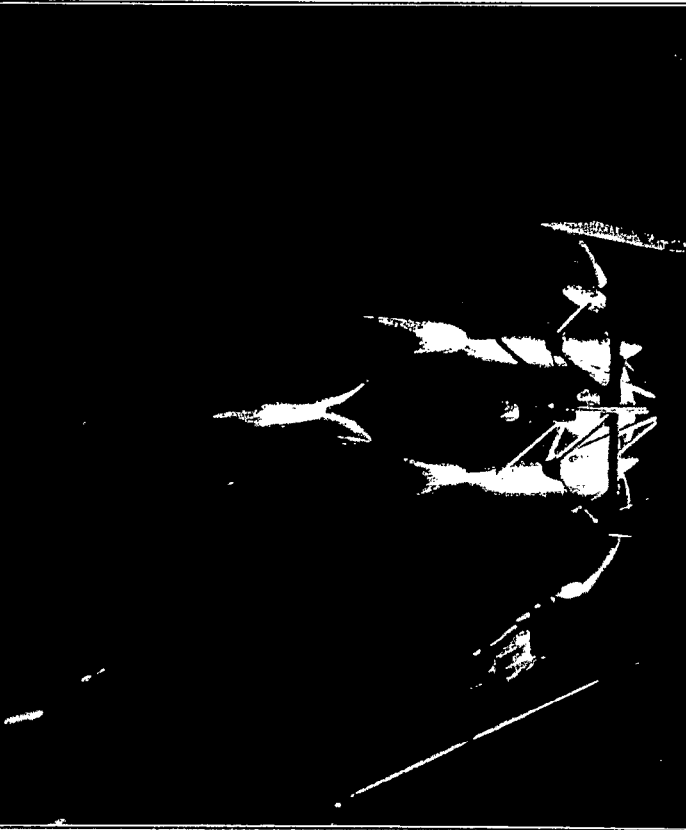


Fig. 19 Formation of waves about V-bottom, pointed float at low speed. Length of model 1.1 m, velocity 2.45 m/s



Fig. 20 Formation of waves about flat float on the step. Length of model 1 m, speed 6.09 m/s



Fig. 21 Formation of waves about pointed V-bottom float on the step. Length of model 1.1 m, speed 6.08 m/s

